

## Imaging and analysis

Motor units and neuromuscular junctions were reconstructed on laser scanning confocal microscopes (Olympus Flouview FV500 and Bio-Rad 1024). Images were obtained with a  $\times 60$  (1.4 NA) oil objective with a zoom equal to 2 for motor unit reconstructions and zoom equal to 4 for diffraction-limited imaging of individual junctions. YFP was excited with the 488 nm line of an argon laser and detected with a 520–550 nm band-pass emission filter. CFP was excited with the 442 nm line of an HeCd laser and detected with a 465–495 nm band-pass emission filter. Alexa-594  $\alpha$ -bungarotoxin was excited by using the 568 nm line of a Krypton laser and detected with a 585 long-pass barrier filter. Z-steps were 0.6  $\mu\text{m}$  for motor unit reconstructions and 0.3  $\mu\text{m}$  for high-resolution imaging of individual junctions.

Z-stacks were flattened by using a two-dimensional maximum projection algorithm in MetaMorph (Universal Imaging Corporation), and montages of the 20–50 stacks that constitute a motor unit were aligned with Adobe Photoshop. Percentage occupancy at individual junctions was determined in MetaMorph by counting the number of YFP (or CFP) pixels overlying receptors labelled with Alexa-594-conjugated  $\alpha$ -bungarotoxin. Axon diameter was determined, by using MetaMorph, as the width of the innervating CFP or YFP axon 10  $\mu\text{m}$  from the edge of the endplate where the axon enters. Branch number was determined by constructing complete branch diagrams of the motor units of interest and counting the number of branch points between the cell body and a particular junction.

Pair-wise statistical comparisons between motor units (i.e. CFP occupancy versus YFP occupancy) were done by using a non-parametric Mann–Whitney non-directional test. Distributions of histograms (Fig. 3 and Supplementary Fig. 1) were compared by using a Kolmogorov–Smirnov (K–S) goodness-of-fit test with S-Plus 4, MathSoft. We used a Monte Carlo simulation (column b, Fig. 2) to test whether the distribution of synaptic occupancy of a specific cohort of junctions facing the same competitor was different than the overall distribution of synaptic occupancy of the motor unit containing that cohort. As the most striking characteristic of the co-innervated junctions was their apparent similarity to each other, we compared the standard deviation of synaptic occupancy of junctions or axon diameter within the cohort with the standard deviation of the entire motor unit. Specifically, one trial of the Monte Carlo simulation randomly selected the same number of junctions from the entire motor unit as observed in the co-innervated cohort, and the standard deviation of that random sample was calculated (program written by S. Turney for Matlab). The process was repeated 100,000 times. The probability that the homogeneity occurring within a cohort could have occurred by chance was taken as the percentage of randomly selected samples that had an equal or smaller standard deviation than the cohort.

Received 5 February; accepted 2 June 2003; doi:10.1038/nature01836.

- Purves, D. & Lichtman, J. W. Elimination of synapses in the developing nervous system. *Science* **210**, 153–157 (1980).
- Wong, R. O. L. & Lichtman, J. W. in *Fundamental Neuroscience* (ed. Squire, L. et al.) 533–553 (Academic, San Diego, 2003).
- Keller-Peck, C. R. et al. Asynchronous synapse elimination in neonatal motor units: studies using GFP transgenic mice. *Neuron* **31**, 381–394 (2001).
- Buffelli, M. et al. Genetic evidence that relative synaptic efficacy biases the outcome of synaptic competition. *Nature*, this issue (2003).
- Lichtman, J. W. The reorganization of synaptic connections in the rat submandibular ganglion during post-natal development. *J. Physiol. (Lond.)* **273**, 155–177 (1977).
- Colman, H., Nabekura, J. & Lichtman, J. W. Alterations in synaptic strength preceding axon withdrawal. *Science* **275**, 356–361 (1997).
- Chen, C. & Regehr, W. G. Developmental remodeling of the retinogeniculate synapse. *Neuron* **28**, 955–966 (2000).
- Brown, M. C., Jansen, J. K. & Van Essen, D. C. Polyneuronal innervation of skeletal muscle in newborn rats and its elimination during maturation. *J. Physiol. (Lond.)* **261**, 387–422 (1976).
- Jansen, J. K. & Fladby, T. The perinatal reorganization of the innervation of skeletal muscle in mammals. *Prog. Neurobiol.* **34**, 39–90 (1990).
- Sanes, J. R. & Lichtman, J. W. Development of the vertebrate neuromuscular junction. *Annu. Rev. Neurosci.* **22**, 389–442 (1999).
- Feng, G. et al. Imaging neuronal subsets in transgenic mice expressing multiple spectral variants of GFP. *Neuron* **28**, 41–51 (2000).
- Press, W. H., Teukolsky, S. A., Vetterling, W. T. & Flannery, B. P. *Numerical Recipes in C* (Cambridge Univ. Press, 1992).
- Gan, W. B. & Lichtman, J. W. Synaptic segregation at the developing neuromuscular junction. *Science* **282**, 1508–1511 (1998).
- Personius, K. E. & Balice-Gordon, R. J. Activity-dependent editing of neuromuscular synaptic connections. *Brain Res. Bull.* **53**, 513–522 (2000).
- Balice-Gordon, R. J. & Lichtman, J. W. Long-term synapse loss induced by focal blockade of postsynaptic receptors. *Nature* **372**, 519–524 (1994).
- Buffelli, M., Busetto, G., Cangiano, L. & Cangiano, A. Perinatal switch from synchronous to asynchronous activity of motoneurons: link with synapse elimination. *Proc. Natl Acad. Sci. USA* **99**, 13200–13205 (2002).
- Personius, K. E. & Balice-Gordon, R. J. Loss of correlated motor neuron activity during synaptic competition at developing neuromuscular synapses. *Neuron* **31**, 395–408 (2001).
- Barber, M. J. & Lichtman, J. W. Activity-driven synapse elimination leads paradoxically to domination by inactive neurons. *J. Neurosci.* **19**, 9975–9985 (1999).
- Walsh, M. K. & Lichtman, J. W. In vivo time lapse imaging of synaptic takeover associated with naturally occurring synapse elimination. *Neuron* **37**, 1–7 (2003).

Supplementary Information accompanies the paper on [www.nature.com/nature](http://www.nature.com/nature).

**Acknowledgements** We thank the members of our laboratory and J. R. Sanes for many useful discussions, J. Tollet for help breeding animals, J. D. Wiley for assistance in collecting initial data, and S. Turney for technical advice and developing programs for the statistical tests. We thank J. R. Sanes and G. Feng for generating the original transgenic mice. This work was supported by grants from the National Institutes of Health and the Muscular Dystrophy Association to J.W.L., and by support from the Bakewell Neuroimaging Fund.

**Competing interests statement** The authors declare that they have no competing financial interests.

**Correspondence** and requests for materials should be addressed to J.W.L. (jeff@pcg.wustl.edu).

## Genetic evidence that relative synaptic efficacy biases the outcome of synaptic competition

Mario Buffelli\*†, Robert W. Burgess\*‡, Guoping Feng\*‡, Corrinne G. Lobe§, Jeff W. Lichtman\* & Joshua R. Sanes\*

\* Department of Anatomy and Neurobiology, Washington University School of Medicine, 660 South Euclid, St Louis, Missouri 63110, USA

† Dipartimento di Scienze Neurologiche e della Visione, Università degli Studi di Verona, Via dell' Artiglierie 8, 37129 Verona, Italy

§ Sunnybrook and Women's College Health Science Centre, 2075 Bayview, Toronto, Ontario M4N 3M5, Canada

Synaptic activity drives synaptic rearrangement in the vertebrate nervous system; indeed, this appears to be a main way in which experience shapes neural connectivity<sup>1,2</sup>. One rearrangement that occurs in many parts of the nervous system during early post-natal life is a competitive process called 'synapse elimination'<sup>3,4</sup>. At the neuromuscular junction, where synapse elimination has been analysed in detail, muscle fibres are initially innervated by multiple axons, then all but one are withdrawn and the 'winner' enlarges<sup>4–6</sup>. In support of the idea that synapse elimination is activity dependent, it is slowed or speeded when total neuromuscular activity is decreased or increased, respectively<sup>4,7–13</sup>. However, most hypotheses about synaptic rearrangement postulate that change depends less on total activity than on the relative activity of the competitors<sup>1–4,13,14</sup>. Intuitively, it seems that the input best able to excite its postsynaptic target would be most likely to win the competition, but some theories and results make other predictions<sup>14–18</sup>. Here we use a genetic method to selectively inhibit neurotransmission from one of two inputs to a single target cell. We show that more powerful inputs are strongly favoured competitors during synapse elimination.

The only two experiments that have differentially decreased activity of some inputs to a muscle led to opposite conclusions: the more active axon was favoured in one, and the less active in the other<sup>17,18</sup>. To re-examine this issue, we reduced neurotransmission from a subset of motor axons by depleting them of choline acetyltransferase (ChAT), the sole synthetic enzyme for the neurotransmitter, acetylcholine. Neuromuscular junctions (NMJs) form in mutant mice that completely lack ChAT (*ChAT*<sup>−/−</sup>), but electrophysiological recordings showed that no neurotransmission occurs, and the mice die at birth<sup>19,20</sup>. Here, we used a conditional allele of the *ChAT* gene (*ChAT*<sup>lox/lox</sup>), so that we could allow embryogenesis to proceed normally, then inactivate *ChAT* postnatally. Exons near the 5' end of ChAT were flanked by loxP sites; excision by Cre recombinase generated the *ChAT*<sup>−/−</sup> allele<sup>19</sup>. To

‡ Present addresses: Jackson Laboratories, Bar Harbor, Maine 04609, USA (R.W.B.); Department of Neurobiology, Duke University Medical School, Durham, North Carolina 27710, USA (G.F.).

control the timing and magnitude of excision, Cre was fused to the ligand-binding domain of an oestrogen receptor (ER); the ER domain prevents Cre activity, but inhibition is relieved by administration of ligand<sup>21</sup>. To further control Cre activity, the receptor fragment had been mutated to prevent binding of the endogenous ligand (oestradiol) while retaining sensitivity to a synthetic ligand (tamoxifen). In the transgenic mice we used (*CX-CreER*; ref. 22), the Cre-ER fusion was expressed nearly ubiquitously. Thus, we anticipated that administration of tamoxifen to *CX-CreERxChAT<sup>flox/flox</sup>* or *CX-CreERxChAT<sup>flox/-</sup>* pups would inactivate ChAT in subsets of motor neurons, with the number of affected cells being dependent on the dose of tamoxifen administered.

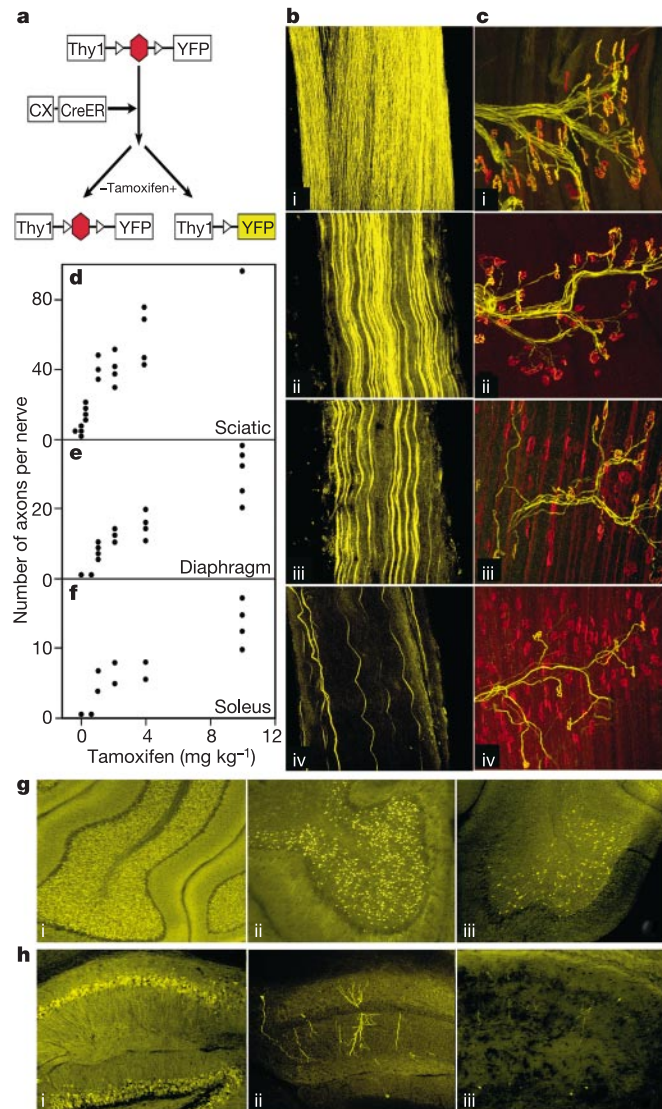


**Figure 1** Activation of gene expression in subsets of motor neurons. **a**, Neuron-specific regulatory elements from the *thy1* gene drive expression of YFP after Cre-mediated excision of a STOP cassette. Cre was fused to the ligand-binding domain of a steroid receptor (CreER), so excision required administration of tamoxifen. **b, c**, Sciatic nerves (**b**) and sternomastoid muscles (**c**) from *Thy1-STOP-YFPxCre* (i) or *Thy1-STOP-YFPxCX-CreER* mice (ii–iv). Tamoxifen was injected at 10 mg kg<sup>-1</sup> (ii), 4 mg kg<sup>-1</sup> (iii) or 0.5 mg kg<sup>-1</sup> (iv), 10–15 d before analysis. Muscles in (**c**) were stained with anti-GFP plus rhodamine  $\alpha$ -bungarotoxin to label the acetylcholine receptors at endplates. **d–f**, YFP-positive axons as a function of tamoxifen dose in *Thy1-STOP-YFPxCX-CreER* mice. Each point represents one muscle or nerve. **g, h**, Cerebella (**g**) and hippocampi (**h**) from *Thy1-STOP-YFPxCX-CreER* mice injected with 10 mg kg<sup>-1</sup> (i), 1 mg kg<sup>-1</sup> (ii) or 0 mg kg<sup>-1</sup> (iii) tamoxifen. At the lowest doses of tamoxifen, Golgi-like labelling of individual hippocampal neurons is evident. Fewer than 1% of granule cells are labelled without tamoxifen.

To test this strategy, we first generated transgenic mice in which expression of a yellow fluorescent protein (YFP) in neurons<sup>23</sup> was completely dependent on Cre-mediated excision of inhibitory (STOP) sequences (Fig. 1a). We mated these *Thy1-STOP-YFP* mice to mice in which constitutively active Cre was expressed throughout the embryo (*A-Cre*; ref. 24) and selected lines in which all motor axons of *Thy1-STOP-YFPxCre* offspring were YFP-positive (Fig. 1b(i)). These lines were then used to test the ability of the *CX-CreER* transgene to act in motor neurons. The number of labelled axons in peripheral nerves of *Thy1-STOP-YFPxCX-CreER* mice was proportional to the dose of tamoxifen administered, but the intensity with which individual axons were labelled did not appear to vary with dose (Fig. 1b–f). Expression of YFP in many populations of central neurons was also tamoxifen dependent (Fig. 1g), generating a ‘Golgi-like’ pattern that may be useful for imaging studies. Based on these results, we chose doses of 5 and 100  $\mu$ g (approximately 2.5 and 50 mg kg<sup>-1</sup>, referred to below as ‘low’ and ‘high’) administered on the first postnatal day (P0), to excise floxed sequences in 10–20% or >50% of motor neurons, respectively.

Next, we assessed the ability of the *CX-CreER* transgene to inactivate ChAT. Motor axons were labelled by antibodies to ChAT in *CreERxChAT<sup>flox/flox</sup>* mice without tamoxifen, but labelling was lost after administration of tamoxifen at P0. As expected, 10–20% and >50% of axons in intramuscular nerves of *CX-CreERxChAT<sup>flox/flox</sup>* mice were ChAT-negative (ChAT<sup>-</sup>) 1 week after low and high doses of tamoxifen, respectively (Fig. 2a, b). Similar results were observed in soleus, diaphragm, sternomastoid, serratus anterior, spinotrapezius and extensor digitorum longus muscles. No behavioural abnormalities were detected after administration of the low dose, but mice became noticeably weak by P9 and died at P14–15 after administration of the high dose. Importantly, a high dose of tamoxifen neither led to weakness nor affected neuromuscular morphology in *CX-CreERxChAT<sup>flox/+</sup>* or *CX-CreERxThy1-STOP-YFP* mice (data not shown).

Based on these results, we assessed NMJs at P11 in *CX-CreERxChAT<sup>flox/flox</sup>* mice that had received a low dose of tamoxifen at P0. In the muscles examined, all muscle fibres are multiply innervated at P0, then lose inputs during the first two postnatal weeks<sup>4,5</sup>. Most NMJs have already completed synapse elimination by P11, but we chose this age for two reasons: (1) by immunohistochemical criteria, most axons were unambiguously either ChAT<sup>+</sup> or ChAT<sup>-</sup> by this time; (2) at this age, the ‘winning’ and ‘losing’ inputs can be predicted with ~80% accuracy by assessing which occupies more territory (ref. 6 and M. K. Walsh, personal communication). Whole muscles were triply labelled with fluorescent- $\alpha$ -bungarotoxin (which binds to acetylcholine receptors in the postsynaptic membrane), antibodies to ChAT, and a mixture of antibodies to neurofilaments (to label axons) and a synaptic vesicle protein (to label motor nerve terminals). NMJs were imaged in whole mounts and reconstructed by confocal microscopy.

The main result is illustrated in Fig. 2c, which shows a group of three neighbouring NMJs from a low dose *CX-CreERxChAT<sup>flox/flox</sup>* mouse. This group was unusual in that all three NMJs were doubly innervated, even though ~80% of the fibres in this muscle were already singly innervated. At two of the NMJs, one axon was ChAT<sup>+</sup> and the other was ChAT<sup>-</sup>. Knowing that the two axons occupy largely non-overlapping territories at this stage (see Table 1 in ref. 25), we compared the ChAT-stained area of the terminal arbor (representing the ChAT<sup>+</sup> territory) with the neurofilament and vesicle-positive area (representing both axons). At both of these synapses, the ChAT<sup>+</sup> axon occupied more than half of the area occupied by both axons together: 75% in the NMJ shown at higher power in Fig. 2d, and 81% in its neighbour. The average occupancy by ChAT<sup>+</sup> axons at such doubly innervated sites was 84.9  $\pm$  2.2% (mean  $\pm$  s.e.m.,  $n = 29$  synapses from four muscles). Similar results (82  $\pm$  2.1% occupancy) were obtained when the area of the ChAT<sup>+</sup> axons was expressed as a fraction of the acetylcholine

receptor-rich area rather than as a fraction of the total presynaptic arbor. By either measure, the ChAT<sup>+</sup> axon occupied more than 50% of the site at all 29 synapses (Fig. 2g; non-random at  $P \ll 0.001$  by  $\chi^2$  test). Similar results were obtained after tamoxifen injection at P2 (data not shown).

These results imply that relative efficacy biases the outcome of synaptic competition. Before drawing this conclusion, however, we considered two alternative explanations. First, ChAT<sup>-</sup> axons were in the minority, and it was possible that successful axons were those whose activity level conformed most closely to the average level in the target field (a 'democratic' model). Second, inactive axons might be intrinsically incompetent to maintain a synapse, regardless of whether or not they were pitted against a more active axon. To address these possibilities, we confocally reconstructed synapses from high-dose *CX-CreERxChAT<sup>fllox/fllox</sup>* mice, in which most axons were ChAT<sup>-</sup> (Fig. 2e). At all synapses innervated by a ChAT<sup>+</sup> and a

ChAT<sup>-</sup> axon, the ChAT<sup>+</sup> axon occupied more than 50% of the site (average  $79.9 \pm 5.8\%$ ; Fig. 2h), indicating that activity level predicted outcome whereas majority status did not. Moreover, multiple innervation was more prevalent in these muscles than in controls (Fig. 2i), and numerous sites were innervated by two ChAT<sup>-</sup> axons, consistent with previous results from globally paralysed muscles<sup>6,8,11</sup>, but inconsistent with the idea that all ChAT<sup>-</sup> axons withdraw from synapses. ChAT<sup>-</sup> axons also fully occupied synaptic sites at singly innervated NMJs; in these cases, competition may have been underway or complete before ChAT was lost. Thus, inactive axons are capable of maintaining synaptic territory, but appear to be hampered from doing so in the presence of an active competitor.

A second aspect of the competitive process allowed us to further test the idea that ChAT<sup>-</sup> axons fare poorly not because they are inactive, but rather because they are pitted against more efficacious

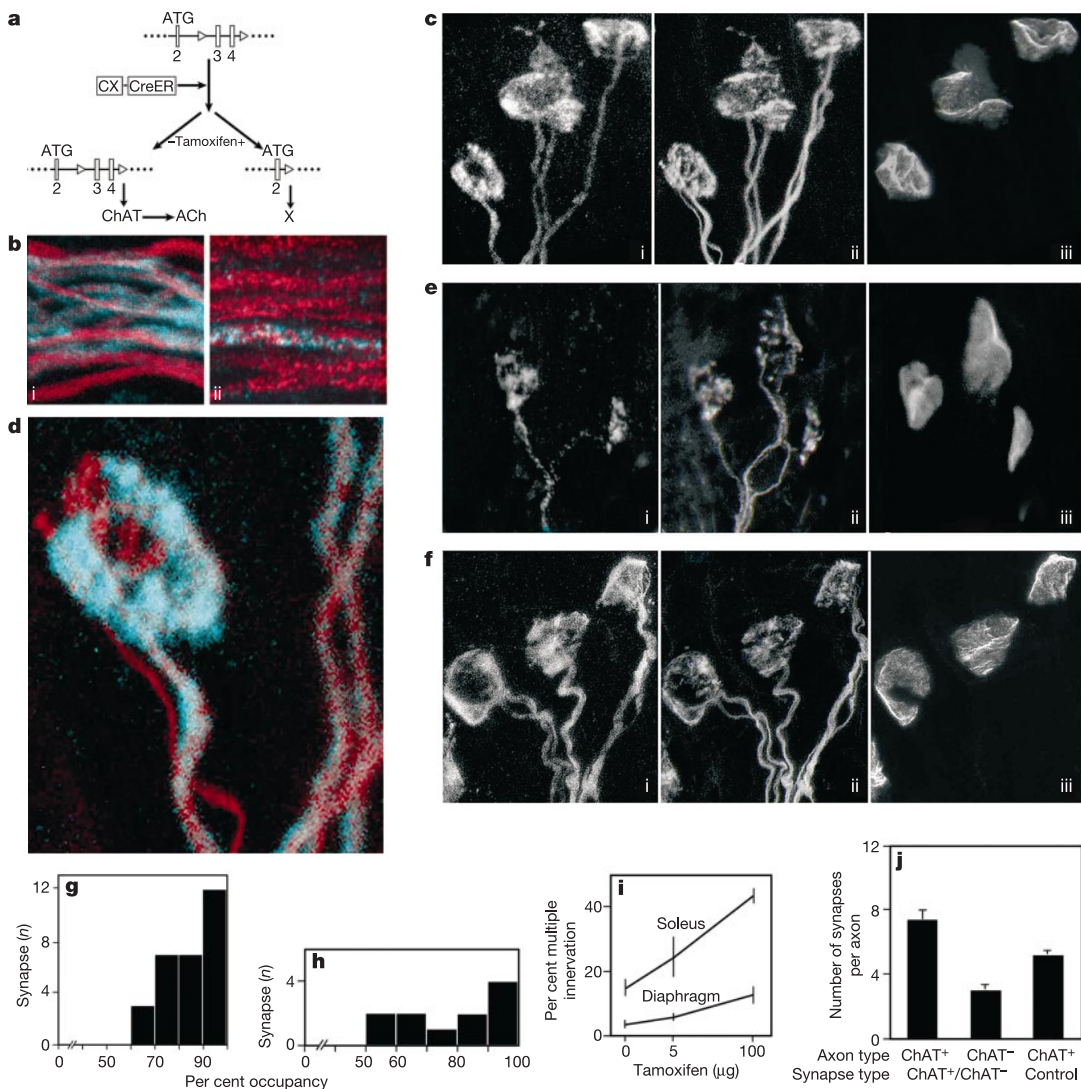


**Figure 2** ChAT<sup>+</sup> axons are favoured competitors over ChAT<sup>-</sup> axons at multiply innervated neuromuscular junctions. **a**, The conditional *Chat* allele (*Chat<sup>fllox/fllox</sup>*), and the null allele<sup>19</sup> generated by Cre-mediated excision after tamoxifen administration to *CX-CreERxChAT<sup>fllox/fllox</sup>* mice. **b**, Nerve branches from *CX-CreERxChAT<sup>fllox/fllox</sup>* mice treated with 5 μg (**i**) or 100 μg (**ii**) tamoxifen at P0, then stained for neurofilaments (red) and ChAT (blue) at P11. **c–f**, neuromuscular junctions (NMJs) from *CX-CreERxChAT<sup>fllox/fllox</sup>* mice administered 5 μg (**c, d**) or 100 μg (**e, f**) tamoxifen or saline (**f**) at P0, then triply stained for axons (**i**), ChAT (**ii**) and acetylcholine receptors (**iii**) at P11. ChAT (blue) and axon (red) staining from one NMJ are overlaid in **d, g, h**. Fraction of the synaptic site occupied by the

ChAT<sup>+</sup> axon at NMJs co-occupied by a ChAT<sup>+</sup> and a ChAT<sup>-</sup> axon after administration of 5 μg (**g**) or 100 μg (**h**) tamoxifen. The ChAT-positive axon occupied more than 50% of all sites. **i**, Percentage of NMJs that were doubly innervated at P11 in soleus or diaphragm muscles from *CX-CreERxChAT<sup>fllox/fllox</sup>* mice administered 0, 5 or 100 μg tamoxifen at P0. Bars indicate range;  $\geq 100$  NMJs were counted from each muscle. **j**, Synaptic territory of ChAT<sup>+</sup> or ChAT<sup>-</sup> axons, calculated as the ratio of the number of NMJs innervated by each category of axon to the number of axons of that category in an intramuscular nerve branch. (Mean  $\pm$  s.e.m. for 10–18 microscope (20 $\times$ ) fields.)

opponents. During naturally occurring synapse elimination, the axon branch leading to the 'losing' terminal atrophies as or before the terminal branches withdraw<sup>25,26</sup>. We therefore measured the calibre of pre-terminal axons in *CX-CreERxChAT<sup>fllox/fllox</sup>* mice. At synapses innervated by a ChAT<sup>+</sup> and a ChAT<sup>-</sup> axon, the ChAT<sup>+</sup> axon was usually thicker and never thinner than the ChAT<sup>-</sup> axon, providing an additional line of support for the conclusion that impotent axons fare poorly in the competition (Fig. 3a-c). More importantly, the difference between the diameters of the two inputs was greater at NMJs innervated by a ChAT<sup>+</sup> and a ChAT<sup>-</sup> axon (where activity differences between inputs were maximized) than at NMJs innervated by two ChAT<sup>-</sup> axons (where activity differences between inputs should be less) (Fig. 3d). This result does not reflect

a general atrophy of ChAT<sup>-</sup> axons, because the average diameter of axons at synapses with two ChAT<sup>-</sup> inputs was similar to that at synapses with two ChAT<sup>+</sup> inputs (Fig. 3e). Moreover, axons at synapses innervated by two ChAT<sup>+</sup> or two ChAT<sup>-</sup> inputs were on average thinner than the ChAT<sup>+</sup> axons and thicker than the ChAT<sup>-</sup> axons at synapses with one input of each type. In other words, a ChAT<sup>-</sup> axon fared worse when confronting a normally active axon than when confronting another weak input. This result shows that the size of an axon branch is influenced by the identity of the competing input, implying that strong inputs destabilize weaker inputs to a common postsynaptic target.

Finally, we tested the prediction that, if active inputs out-compete less active inputs, active motor axons should come to innervate more muscle fibres than inactive motor axons. We had no way of determining the absolute size of motor units, so we counted, in multiple microscope fields, the numbers of ChAT<sup>+</sup> and ChAT<sup>-</sup> axons in intramuscular nerves and the numbers of NMJs with ChAT<sup>+</sup> or ChAT<sup>-</sup> terminals. By this measure, each ChAT<sup>+</sup> axon innervates over twice as many synaptic sites as each ChAT<sup>-</sup> axon (Fig. 2i; only one NMJ in this data set was innervated by both a ChAT<sup>+</sup> and a ChAT<sup>-</sup> axon). The number of NMJs per axon in control muscles, measured in the same way, was intermediate between these values. This result confirms the inference that differences in efficacy bias not only the progress of competition at individual sites, but also the outcome of that competition.

In summary, we have directly tested the influential hypothesis<sup>1-18</sup> that differential efficacy affects the competitive processes that result in the elimination of supernumerary synapses during early postnatal life. The test relied on three techniques. First, targeting of ChAT allowed us to decrease neurotransmission specifically, without affecting other aspects of axonal physiology such as propagation of action potentials. Second, the tamoxifen-Cre system allowed us to inactivate some inputs to a muscle, or even to a single postsynaptic cell, without perturbing neighbouring inputs. Importantly, in the 'low dose' animals, ChAT<sup>-</sup> axons were in a small minority, so potentially complicating global effects on activity were inconsequential. Third, confocal imaging allowed us to measure synaptic occupancy on individual postsynaptic cells, rather than inferring occupancy from electrical or mechanical measurements as has been done previously<sup>17,18</sup>. By combining these methods, we showed for the first time that the more powerful input to a synaptic target cell destabilizes a less powerful input to the same target. It remains to be determined whether the timing and pattern of neurotransmission, as well as its total amount, influence the outcome of this competitive process<sup>1,2,13,14,27,28</sup>.

Our results leave open the question of whether activity is the predominant driver of synapse elimination under normal circumstances, or whether it plays more subtle roles. If activity predominates, one might imagine that all synapses at which branches of the same two axons compete would proceed along the same path to the same outcome. Moreover if motor units in normal muscles have limited resources, larger motor units might release less transmitter at each synapse and be at a competitive disadvantage. A companion study<sup>25</sup> confirms both predictions. Taken together, those results and ours lead to the surprising idea that inter-axonal differences in the ability to an axon to activate a target (reflecting levels or patterns of axonal activity and the amount of transmitter each impulse releases) can completely account for the tempo and outcome of some synaptic rearrangements. □

Methods

Mice

Transgenic mice expressing YFP under the control of neuron-specific regulatory elements from the murine *thy-1* gene are described in ref. 23. To generate transgenic mice that expressed YFP conditionally, we modified the vector by inserting a 'lox-stop-lox' cassette<sup>29</sup> upstream of the first codon of YFP. Transgenic mice expressing Cre under the control of regulatory sequences from the  $\beta$ -actin gene (*A-Cre*) were a gift from G. Martin (University of

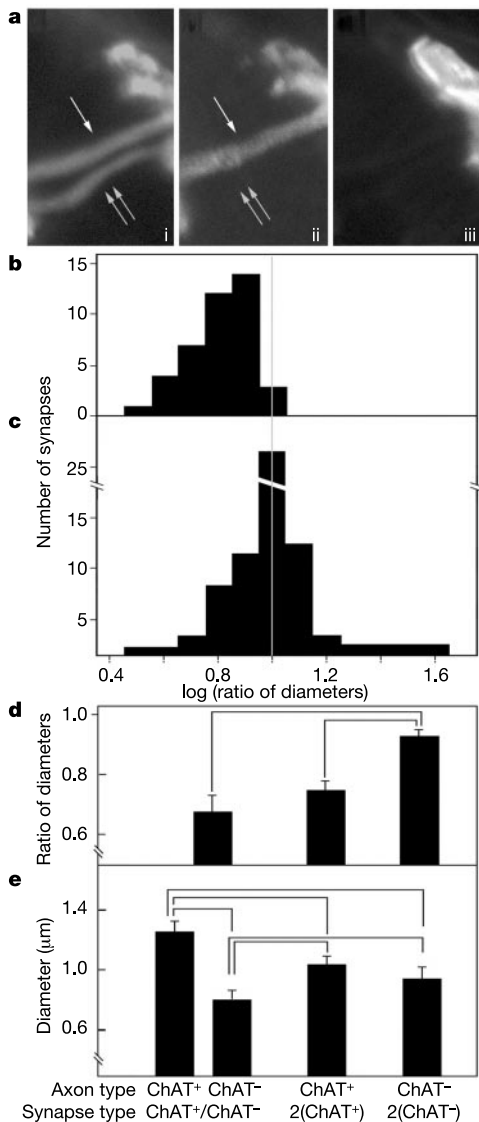


**Figure 3** ChAT<sup>-</sup> axons fare worse when pitted against a ChAT<sup>+</sup> axon than when pitted against another ChAT<sup>-</sup> axon. **a**, Pre-terminal axons at an NMJ innervated by a ChAT<sup>+</sup> and a ChAT<sup>-</sup> axon, triply labelled as in Fig. 2c-f. The ChAT<sup>+</sup> axon is thicker than the ChAT<sup>-</sup> axon. **b**, Ratio of the pre-terminal diameter of the ChAT<sup>-</sup> axon to that of the ChAT<sup>+</sup> axon at synaptic sites co-occupied by one axon of each type. **c**, Similar measurements of ratio of diameters of thin to thick axons at sites in the same muscles co-occupied by two ChAT<sup>+</sup> or two ChAT<sup>-</sup> axons. At each site, one diameter was assigned at random as the numerator. **d, e**, Pre-terminal diameters of axons co-occupying individual synaptic sites (**e**), and ratio of the diameter of the thinner axon at each site to that of the thicker (**d**). Values joined by horizontal lines differ from each other at *P* < 0.05 by Student's *t*-test. Analysis is based on 40 ChAT<sup>+</sup>/ChAT<sup>-</sup>, 45 ChAT<sup>+</sup>/ChAT<sup>+</sup> and 18 ChAT<sup>-</sup>/ChAT<sup>-</sup> synapses.

California at San Francisco)<sup>24</sup>. Transgenic mice expressing Cre-ER nearly ubiquitously under the control of hybrid viral and actin regulatory elements (*CX-CreER*) are described in ref. 22.

To target the *ChAT* locus, exons 3 and 4 were flanked by loxP sites and a *Neo* gene was introduced in the intron between exons 4 and 5 (ref. 19). In ref. 19, we showed that excision of these exons in the germline by mating to *A-Cre* mice generated a null allele in subsequent generations, in which no ChAT protein or activity was detectable. Because we were concerned that the presence of foreign sequences in the *ChAT* locus might interfere with ChAT expression, the *Neo* gene was flanked by Frt sites, so that it could be excised by mating to mice in which Flp recombinase was expressed ubiquitously<sup>30</sup>. However, we detected no difference in phenotype between mice that retained or lacked the *Neo* gene. All mice were maintained in a C57/B6 background. Tamoxifen (Sigma) was dissolved in 0.1% ethanol, 99% corn oil for intraperitoneal injection.

## Imaging

Mice were perfused with 2% paraformaldehyde, then muscles were dissected, postfixed for 30 min in the same solution, and treated successively with 0.1M glycine, 0.5% Triton-X-100 (2 h) and 4% bovine serum albumin, 0.5% Triton-X-100 in PBS (2 h; blocking solution). They were then stained for 24 h with primary antibodies (mouse anti-neurofilament (Sternberger), mouse anti-SV2 (Developmental Studies Hybridoma Bank) and goat anti-ChAT (Chemicon)), washed for 24–48 h, stained for 24 h with fluorescent reagents (Alexa 594–donkey anti mouse IgG, Alexa 488–donkey anti-goat IgG, and Alexa 647- $\alpha$ -bungarotoxin, all from Molecular Probes), washed for 24 h, and mounted. Stacks of images were collected at intervals of 0.35–0.5  $\mu$ m with a confocal microscope, then reconstructed in Metamorph (Universal Imaging) and rendered in Photoshop (Adobe).

Received 5 February; accepted 2 June 2003; doi:10.1038/nature01844.

- Katz, L. C. & Shatz, C. J. Synaptic activity and the construction of cortical circuits. *Science* **274**, 1133–1138 (1996).
- Sengpiel, F. & Kind, P. C. The role of activity in development of the visual system. *Curr. Biol.* **12**, R818–R826 (2002).
- Lichtman, J. W. & Colman, H. Synapse elimination and indelible memory. *Neuron* **25**, 269–278 (2000).
- Personius, K. E. & Balice-Gordon, R. J. Activity-dependent synaptic plasticity: insights from neuromuscular junctions. *Neuroscientist* **8**, 414–422 (2002).
- Sanes, J. R. & Lichtman, J. W. Development of the vertebrate neuromuscular junction. *Annu. Rev. Neurosci.* **22**, 389–442 (1999).
- Walsh, M. K. & Lichtman, J. W. In vivo time-lapse imaging of synaptic takeover associated with naturally occurring synapse elimination. *Neuron* **37**, 67–73 (2003).
- Benoit, P. & Changeux, J. P. Consequences of tenotomy on the evolution of multi-innervation in developing rat soleus muscle. *Brain Res.* **99**, 354–358 (1975).
- Thompson, W., Kuffler, D. P. & Jansen, J. K. The effect of prolonged, reversible block of nerve impulses on the elimination of polyneuronal innervation of new-born rat skeletal muscle fibers. *Neuroscience* **4**, 271–281 (1979).
- Ding, R., Jansen, J. K., Laing, N. G. & Tonnesen, H. The innervation of skeletal muscles in chickens curarized during early development. *J. Neurocytol.* **12**, 887–919 (1983).
- Thompson, W. Synapse elimination in neonatal rat muscle is sensitive to pattern of muscle use. *Nature* **302**, 614–616 (1983).
- Duxson, M. J. The effect of postsynaptic block on development of the neuromuscular junction in postnatal rats. *J. Neurocytol.* **11**, 395–408 (1982).
- O'Brien, R. A., Ostberg, A. J. & Vrbova, G. Observations on the elimination of polyneuronal innervation in developing mammalian skeletal muscle. *J. Physiol. (Lond.)* **282**, 571–582 (1978).
- Busetto, G., Buffelli, M., Tognana, E., Bellico, F. & Cangiano, A. Hebbian mechanisms revealed by electrical stimulation at developing rat neuromuscular junctions. *J. Neurosci.* **20**, 685–695 (2000).
- Barber, M. J. & Lichtman, J. W. Activity-driven synapse elimination leads paradoxically to domination by inactive neurons. *J. Neurosci.* **19**, 9975–9985 (1999).
- Hata, Y., Tsumoto, T. & Stryker, M. P. Selective pruning of more active afferents when cat visual cortex is pharmacologically inhibited. *Neuron* **22**, 375–381 (1999).
- Costanzo, E. M., Barry, J. A. & Ribchester, R. R. Competition at silent synapses in reinnervated skeletal muscle. *Nature Neurosci.* **3**, 694–700 (2000).
- Ridge, R. M. & Betz, W. J. The effect of selective, chronic stimulation on motor unit size in developing rat muscle. *J. Neurosci.* **4**, 2614–2620 (1984).
- Callaway, E. M., Soha, J. M. & Van Essen, D. C. Competition favouring inactive over active motor neurons during synapse elimination. *Nature* **328**, 422–426 (1987).
- Misgeld, T. et al. Roles of neurotransmitter in synapse formation: development of neuromuscular junctions lacking choline acetyltransferase. *Neuron* **36**, 635–648 (2002).
- Brandon, E. P., Lin, W., D'Amour, K. A., Pizzo, D. P., Dominguez, B., Sugiura, Y., Thode, S., Ko, C. P., Thal, L. J., Gage, F. H. & Lee, K. F. Aberrant patterning of neuromuscular synapses in choline acetyltransferase-deficient mice. *J. Neurosci.* **23**, 539–549 (2003).
- Metzger, D. & Chambon, P. Site- and time-specific gene targeting in the mouse. *Methods* **24**, 71–80 (2001).
- Guo, C., Yang, W. & Lobe, C. G. A Cre recombinase transgene with mosaic, widespread tamoxifen-inducible action. *Genesis* **32**, 8–18 (2002).
- Feng, G. et al. Imaging neuronal subsets in transgenic mice expressing multiple spectral variants of GFP. *Neuron* **28**, 41–51 (2000).
- Lewandoski, M. & Martin, G. R. Cre-mediated chromosome loss in mice. *Nature Genet.* **17**, 223–225 (1997).
- Kasthuri, N. & Lichtman, J. W. The role of neuronal identity in synaptic competition. *Nature* **424**, 426–430 (2003).
- Keller-Peck, C. R., Walsh, M. K., Gan, W. B., Feng, G., Sanes, J. R. & Lichtman, J. W. Asynchronous synapse elimination in neonatal motor units: studies using GFP transgenic mice. *Neuron* **31**, 381–394 (2001).
- Personius, K. E. & Balice-Gordon, R. J. Loss of correlated motor neuron activity during synaptic competition at developing neuromuscular synapses. *Neuron* **31**, 395–408 (2001).
- Buffelli, M., Busetto, G., Cangiano, L. & Cangiano, A. Perinatal switch from synchronous to

asynchronous activity of motoneurons: link with synapse elimination. *Proc. Natl Acad. Sci. USA* **99**, 13200–13205 (2002).

- Lakso, M. et al. Targeted oncogene activation by site-specific recombination in transgenic mice. *Proc. Natl Acad. Sci. USA* **89**, 6232–6236 (1992).
- Rodriguez, C. I. et al. High-efficiency deleter mice show that FLPe is an alternative to Cre-loxP. *Nature Genet.* **25**, 139–140 (2000).

**Acknowledgements** We thank T. Misgeld and J. Weiner for comments, and R. Lewis for assistance. This work was supported by grants from the National Institutes of Health to J.R.S. and J.W.L.

**Competing interests statement** The authors declare that they have no competing financial interests.

**Correspondence** and requests for materials should be addressed to J.R.S. (sanesj@pcg.wustl.edu).

## Anandamide and arachidonic acid use epoxyeicosatrienoic acids to activate TRPV4 channels

Hiroyuki Watanabe\*†, Joris Vriens\*†, Jean Prenen\*, Guy Droogmans\*, Thomas Voets\* & Bernd Nilius\*

\* Department of Physiology, Campus Gasthuisberg, KU Leuven, B-3000 Leuven, Belgium

† These authors contributed equally to this work

TRPV4 is a widely expressed cation channel of the 'transient receptor potential' (TRP) family<sup>1</sup> that is related to the vanilloid receptor VR1 (TRPV1). It functions as a Ca<sup>2+</sup> entry channel<sup>2</sup> and displays remarkable gating promiscuity by responding to both physical stimuli (cell swelling, innocuous heat<sup>2–7</sup>) and the synthetic ligand 4 $\alpha$ PDD<sup>8</sup>. An endogenous ligand for this channel has not yet been identified. Here we show that the endocannabinoid anandamide and its metabolite arachidonic acid activate TRPV4 in an indirect way involving the cytochrome P450 epoxygenase-dependent formation of epoxyeicosatrienoic acids. Application of 5',6'-epoxyeicosatrienoic acid at submicromolar concentrations activates TRPV4 in a membrane-delimited manner and causes Ca<sup>2+</sup> influx through TRPV4-like channels in vascular endothelial cells. Activation of TRPV4 in vascular endothelial cells might therefore contribute to the relaxant effects of endocannabinoids and their P450 epoxygenase-dependent metabolites on vascular tone<sup>9–12</sup>.

To search for potential endogenous activators of TRPV4, we monitored cytoplasmic free Ca<sup>2+</sup> concentration ([Ca<sup>2+</sup>]<sub>i</sub>) signals in HEK-293 cells expressing TRPV4 in response to various substances related to 4 $\alpha$ -phorbol-12,13-didecanoate (4 $\alpha$ PDD), a potent synthetic ligand of TRPV4, and to anandamide (arachidonylethanolamide (AEA)), a lipid activator of TRPV1. Arachidonic acid (AA; 10  $\mu$ M), a metabolite of AEA, caused a robust increase in [Ca<sup>2+</sup>]<sub>i</sub> in transfected cells but had only a marginal effect in non-transfected cells (Fig. 1a). The elevation of [Ca<sup>2+</sup>]<sub>i</sub> in TRPV4-transfected cells was inhibited by the TRPV4 blocker ruthenium red (10  $\mu$ M)<sup>8</sup> (Fig. 1b) and depended on extracellular Ca<sup>2+</sup>, indicating that AA activates Ca<sup>2+</sup> entry through TRPV4 channels.

In whole-cell patch-clamp experiments, AA activated a large, outwardly rectifying current in TRPV4-transfected cells but not in non-transfected cells (Fig. 1c, d). This current reversed at positive potentials (+21  $\pm$  3 mV,  $n$  = 42, 30 mM external Ca<sup>2+</sup> concentration ([Ca<sup>2+</sup>]<sub>e</sub>))<sup>7,8</sup>, and was blocked in a highly voltage-dependent manner by ruthenium red (RR). These properties are indistinguishable from those of the current activated by the synthetic TRPV4